

Dynamic response of an elastic bridge loaded by a moving elastic beam with a finite length

Eugenia C. Cojocaru*¹ and Hans Irschik²

¹Linz Center of Mechatronics GmbH, 4040 Linz, Austria

²Institute of Technical Mechanics, Johannes-Kepler University, 4040 Linz, Austria

(Received August 8, 2010, Accepted October 22, 2010)

Abstract. The present paper is concerned with vibrations of an elastic bridge loaded by a moving elastic beam of a finite length, which is an extension of the authors' previous study where the second beam was modeled as a semi-infinite beam. The second beam, which represents a train, moves with a constant speed along the bridge and is assumed to be connected to the bridge by the limiting case of a rigid interface such that the deflections of the bridge and the train are forced to be equal. The elastic stiffness and the mass of the train are taken into account. The differential equations are developed according to the Bernoulli-Euler theory and formulated in a non-dimensional form. A solution strategy is developed for the flexural vibrations, bending moments and shear forces in the bridge by means of symbolic computation. When the train travels across the bridge, concentrated forces and moments are found to take place at the front and back side of the train.

Keywords: bridge dynamics; moving beam; Euler-Bernoulli theory; rigid interface.

1. Introduction

The vibration analysis of structural elements such as elastic beams loaded by moving distributed loads has a considerable importance and has been the subject of numerous investigations in various areas, such as the response of bridges to moving vehicles (Fryba 1999) or the transportation of masses along a carrier structure, e.g. of metal slabs in steel fabrication. Usually, a single force, a train of single forces or a force loading with constant distribution was used as a simplified model for the train to determine the dynamical effects of the traveling loads (Pesterev *et al.* 2003). Some of these studies took also into account the inertial effect of the load masses (Fryba 1999, Lee 1996, Yang 2005, Esmailzadeh 1995). Other works did not take it into account but treated aspects such as the effects of dampers on the dynamic response of bridges (Greco and Santini 2002), the distribution of the loads due to sleepers and ballast layer (Museros 2002), or the resonant vibration under high-speed trains (Li 1999). In more complicated models, when the riding comfort or vehicle response is of concern, the dynamic train-bridge interaction was modeled by a series of lumped masses or bodies connected by springs and dashpots, such as in Fryba (1996), Majka and Hartnett (2008), Xia

* Corresponding author, Senior Researcher, E-mail: eugenia.cojocaru@lcm.at

et al. (2003), Zhang (2001), Yang (2001) and Yau (2009).

In reality, the moving masses themselves which represent the train could be considered as structures with an own stiffness. The stiffness of the old trains is often small, but the modern railway trains show an increasing overall stiffness. To this stiffness only little attention has been paid so far in the literature. For this reason the authors started a few years ago a series of studies, which considered the bending stiffness of the train such as Cojocaru *et al.* (2003, 2004). More recently, Zhang and Zheng (2010) considered the traveling beam as to be connected to the bridge by flexible springs at discrete points.

In the present study, the case of a finite elastic beam, called “the train”, is treated, which moves with constant speed along a simply-supported elastic beam, called the bridge. This paper is an extension of the case of a semi-infinite train from Cojocaru *et al.* (2004). The train is connected to the bridge by means of an interface, which is modeled by the limiting case of a rigid connection such that the deflections of the bridge and the train are forced to be equal. The rigid interface is a first step in modeling the real interface between the bridge and the train and is considered from computational reasons. In extension of the usual model of distributed forces, both the elastic stiffness and the mass of the train are taken into account. In this case the vibrations of the bridge are mainly governed by velocity, bending stiffness and mass of the train, besides the parameters of the bridge. In the present paper, the interest of study is focused on the following phenomenon: when the train travels across the bridge, then at the locations of front and end of the train, the concentrated forces and moments turn out to occur, and bending moments and shear forces in the bridge show a jump at these moving locations.

As also in the authors' other studies, the problem was described in a non-dimensional form in order to cover all possible cases by a single formulation. The non-dimensionalised problem is governed by three similarity- or Pi-numbers, that is the bending stiffness ratio, mass ratio and non-dimensional velocity. For the notion of a Pi-number in similarity methods in engineering dynamics, see e.g. Baker *et al.* (1991). Two sets of fourth-order partial differential equations was developed according to the Bernoulli-Euler theory of beams (Ziegler 1991), one set being valid for the unloaded part of the bridge, the other for the region loaded by the train. The two sets are coupled by means of transition conditions at the location of the front and end of the train. To obtain a rapid convergence, the fourth-order partial differential equations were split into a static and a dynamic part. Only the part of the train that moved on the bridge was considered. The influence of the rest of the convoy was taken into account through a system of loadings which consisted of a transversal force and a couple that acted at the location of the bridge entrance and bridge exit. This system depends on the elastic stiffness of the rail outside the bridge and could be obtained by a substructure method similar to the one given in Cojocaru *et al.* (2003). In order to simplify the computational effort of the problem under consideration, the influence of the rest of the convoy is neglected in the present study, setting the respective transversal force and couple equal to zero.

The symbolic computer codes *Maple 9.5* and *MatLab 7.3* are used to solve the problem under consideration, where the methods of real analysis, linear algebra and numerical methods are combined, as described e.g. by Hirsch and Smale (1974) and Kucharski (2000). The Laplace transform is used to solve the quasi-static boundary value problem. To solve the dynamic part of the problem the Galerkin method is applied, where a Ritz approximation with the modes of the natural bridge vibrations as shape functions is used to express the dynamic deflection of the bridge. Non-dimensional deflection, bending moments and shear forces are depicted, and special emphasis is laid on the concentrated force and moment at the front and the end of the train.

2. Elastic beam travelling on a bridge

A simply-supported straight beam of span L is considered in the bridge model. An Euler-Bernoulli beam model is used to describe the deformation of the bridge. A subscript b is used to denote the corresponding mechanical entities of the bridge, which are described as a function of the axial co-ordinate x measured in the inertial co-ordinate system xOy . The inertial co-ordinate system xOy has the origin at the left end of the bridge and the axial co-ordinate x covers the interval from 0 to L and outside from the bridge, see Fig. 1(a). In the following, $B_b = E_b I_b$ denotes the effective bending stiffness, E_b is the Young's modulus, I_b is the second moment of inertia of the cross-sectional area and A_b is the mass per unit length of the bridge. The deflection, slope, bending moment and shear force of the bridge are denoted by w_b , ϕ_b , M_b and Q_b , respectively.

A finite moving elastic beam of length l_t which represents the "train" is assumed to travel with constant speed v across the bridge, such that the front of the train is located at the distance $s(t)$, also measured from the left end of the bridge, see Fig. 1(a), and to possess an own co-ordinate system located at the front of the train which travels together with the train at the same constant speed v . The length of the train is smaller than the length of the bridge. In the following the subscript t is used to denote the corresponding mechanical entities of the train, see also Fig. 1(a), which are described as a function of the axial co-ordinate ξ and time θ measured in the train-fixed co-ordinate system. The train is assumed to be connected to the bridge by the limiting case of a rigid interface such that the deflections of the bridge and the train are forced to be equal.

The bridge is loaded by a transverse forces n_b , see Fig. 1(b), which represents the pressure that is transmitted by the rigid interface from the train to the bridge. The train is loaded by transverse force $n_t(\xi, \theta)$ which represents the pressure that is transmitted by the rigid interface from the bridge, measured in the train-fixed co-ordinate system, and by the own weight $q_t(\xi, \theta)$, see Fig. 1(b). The influence of the rest of the convoy when the train comes on the bridge is taken into account through a bending moment M_0^t and a shear force Q_0^t that act at the location of the bridge entrance, see Fig. 1(b). For the case that the front of the train leaves the bridge, a system of loadings M_L^t and Q_L^t that acts on the bridge exit is taken into account to model the part of the convoy which leaves the

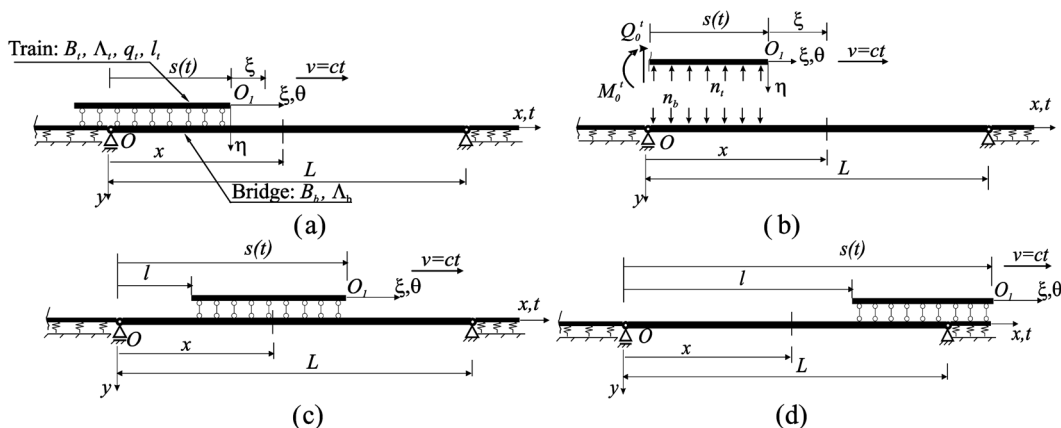


Fig. 1 An elastic bridge loaded by a moving elastic beam with finite length: (a), (b) load case 1, (c) load case 2, (d) load case 3

bridge. The relations between the two co-ordinate systems are

$$x = s(t) + \xi \text{ and } t = \theta \quad (1)$$

where $s(t) = vt$. The governing equation for the undamped flexural vibration of the bridge written in the inertial co-ordinate system, according to Ziegler (1991), are

$$B_b \frac{\partial^4 w_b(x, t)}{\partial x^4} + \Lambda_b \frac{\partial^2 w_b(x, t)}{\partial t^2} = n_b(x, t)[H(x - (s - l)) - H(x - s)] \quad (2)$$

or written in an explicit form

$$\text{- for the loaded part of the bridge: } B_b \frac{\partial^4 w_b(x, t)}{\partial x^4} + \Lambda_b \frac{\partial^2 w_b(x, t)}{\partial t^2} = n_b(x, t) \quad (3)$$

$$\text{- for the unloaded part of the bridge: } B_b \frac{\partial^4 w_b(x, t)}{\partial x^4} + \Lambda_b \frac{\partial^2 w_b(x, t)}{\partial t^2} = 0 \quad (4)$$

The governing equation for the undamped flexural vibration of the train written in the moving coordinate system is

$$B_t \frac{\partial^4 w_t(\xi, \theta)}{\partial \xi^4} + \Lambda_t \frac{\partial^2 w_t(\xi, \theta)}{\partial \theta^2} = q_t(\xi, \theta) - n_t(\xi, \theta) \quad (5)$$

Due to the rigid interface, the deflection of the train at the section ξ should be equal to the deflection of the bridge at the same section, described in the inertial frame xOy . The same is also valid for the contact force between the two beams and for the load of the train

$$\begin{aligned} w_t(\xi, t) &= w_t(x - s(t), t) = w_b(x, t) \\ n_t(\xi, t) &= n_t(x - s(t), t) = n_b(x, t), q_t(\xi, t) = q_t(x - s(t), t)q(x, t) \end{aligned} \quad (6)$$

For the convenience of analysis, using the relationships obtained from the chain rule, see also (Cojocaru *et al.* 2004) and Eq. (6), re-write the governing equation of flexural vibrations of the train from Eq. (4) as a function of the co-ordinate x and t , as follows

$$B_t \frac{\partial^4 w_t(x, t)}{\partial x^4} + \Lambda_t \frac{\partial^2 w_t(x, t)}{\partial t^2} + \Lambda_t \left[2\dot{s} \frac{\partial^2 w_t(x, t)}{\partial x \partial t} + (\dot{s})^2 \frac{\partial^2 w_t(x, t)}{\partial x^2} \right] = -n_b(x, t) + q \quad (7)$$

where $\dot{s}(t)$ equals the velocity v of the train and $\ddot{s}(t)$ is the acceleration of the movement. When the train travels with constant velocity, $\ddot{s}(t) = 0$. In order to simplify the expressions, $s(t)$ is

substituted with s . It is assumed that $q(x,t) = q = g\Lambda t$, with $g = 9.81 \text{ m/s}^2$ the gravitational acceleration. Because the bridge and the train remain all the time in contact and both deflections are equal, the two beams are considered as one beam with bending stiffness $(B_b + B_t)$ and mass $(\Lambda_b + \Lambda_t)$, and the deflection of the system is denoted with $w(x, t)$. Hence, adding Eqs. (3) and (7) yields

$$(B_b + B_t) \frac{\partial^4 w(x, t)}{\partial x^4} + (\Lambda_b + \Lambda_t) \frac{\partial^2 w(x, t)}{\partial t^2} + \Lambda_t \left[2\dot{s} \frac{\partial^2 w(x, t)}{\partial x \partial t} + (\dot{s})^2 \frac{\partial^2 w(x, t)}{\partial x^2} \right] = \Lambda_t g \quad (8)$$

The Eqs. (4) and (8) describe our problem now. Depending on the position of the train on the bridge, three load cases (in a short form denoted as LC) are considered as follows:

- **Load case 1 (LC1)** - $s < L$, $s - l_t < 0$, which means that the train is not entirely on the bridge, see also Fig. 1(a). In this case, the deflection, slope, bending moment and share force of the unloaded part of the bridge in front of the train are denoted as w_f , φ_f , M_f and Q_f , respectively. The boundary conditions (in the following as BC denoted) at the two ends of the beam are defined in terms of displacements and bending moments, as follows

$$w(0, t) = w_f(L, t) = 0$$

$$M(0, t) = -(B_b + B_t) \frac{\partial^2 w(0, t)}{\partial x^2} = M_0', \quad M_f(L, t) = -B_b \frac{\partial^2 w_f(L, t)}{\partial x^2} = 0 \quad (9)$$

where M_0' represents the contribution of the rest of the convoy which still travels outside the bridge on the left end of the bridge. The slope, bending moment and share force of the loaded part of the bridge are denoted by φ , M and Q , respectively.

- **Load case 2 (LC2)** - $s \leq L$, $s - l_t \geq 0$, which means that the train is entirely on the bridge according with Fig. 1(c). Additionally to **LC1**, the deflection, slope, bending moment and share force of the unloaded part of the bridge behind of the train are denoted as w_h , φ_h , M_h and Q_h , respectively. The BCs at the two ends of the beam are defined in terms of displacements and bending moments, as follows

$$w_h(0, t) = w_f(L, t) = 0$$

$$M_h(0, t) = M_f(L, t) = 0 \quad (10)$$

- **Load case 3 (LC3)** - $s > L$, $s - l_t \leq L$, which means that the train is traveling outside of the bridge, see also Fig. 1(d). The BCs at the two ends of the beam are defined in terms of displacements and bending moments, as follows

$$w_h(0, t) = w(L, t) = 0$$

$$M_h(0, t) = -B_b \frac{\partial^2 w_h(0, t)}{\partial x^2} = 0, \quad M(L, t) = -(B_b + B_t) \frac{\partial^2 w(L, t)}{\partial x^2} = M_L' \quad (11)$$

At the front and the end of the train, between the unloaded and loaded part of the bridge, the transition conditions are defined in terms of bending moments and shear forces, as follows:

- for the end (left side) of the train

$$M_h(s-l, t) = -B_b \frac{\partial^2 w_h(s-l, t)}{\partial x^2} = M_{s-l}, \quad Q_h(s-l, t) = -B_b \frac{\partial^3 w_h(s-l, t)}{\partial x^3} = Q_{s-l}$$

$$M(s-l, t) = -(B_b + B_t) \frac{\partial^2 w(s-l, t)}{\partial x^2} = M_{s-l}, \quad Q(s-l, t) = -(B_b + B_t) \frac{\partial^3 w(s-l, t)}{\partial x^3} = Q_{s-l} \quad (12)$$

- for the front (right side) of the train

$$M(s, t) = -(B_b + B_t) \frac{\partial^2 w(s, t)}{\partial x^2} = M_s, \quad Q(s, t) = -(B_b + B_t) \frac{\partial^3 w(s, t)}{\partial x^3} = Q_s$$

$$M_f(s, t) = -B_b \frac{\partial^2 w_f(s, t)}{\partial x^2} = M_s, \quad Q_f(s, t) = -B_b \frac{\partial^3 w_f(s, t)}{\partial x^3} = Q_s \quad (13)$$

The bending moment and shear force in the bridge at the location of the train front are denoted as M_s and Q_s , and train end as M_{s-l} and Q_{s-l} , respectively. At the locations front and end of the train the bending moment and shear force in the unloaded part of the bridge and in the system train+bridge are equal, see Fig. 2(a). Because a rigid interface is assumed between the train and the bridge, the deflection of the train equals the deflection of the bridge, and the second and third derivative of the train beam are not zero at these locations, as showed in Fig. 2(b). Based on these observations it is supposed that at these locations – the front and the end of the train – concentrated forces and moments appear, as shown in Fig. 2(c).

According to the force method (Ziegler 1991), these additional unknowns are calculated from the

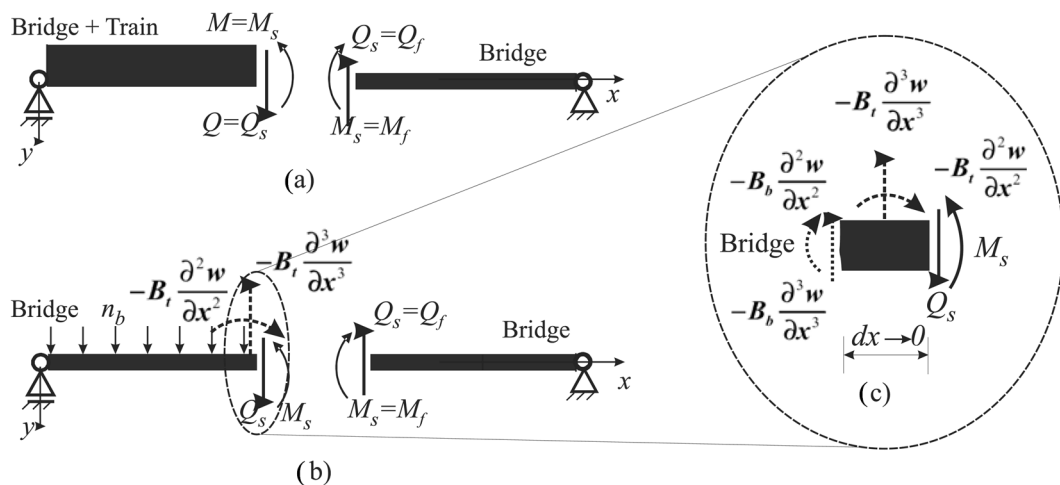


Fig. 2 Equilibrium state at the front and the end of the train

following two conditions of kinematical continuity for the system at the location end and front of the train, respectively

$$\begin{aligned} w_h(x=s-l) &= w(x=s-l), \quad \varphi_h(x=s-l) = \varphi(x=s-l) \\ w(x=s) &= w_f(x=s), \quad \varphi(x=s) = \varphi_f(x=s) \end{aligned} \quad (14)$$

In order to work with minimum number of parameters that determine the solution of the problem, the following dimensionless formulations are introduced

$$\begin{aligned} x=L\hat{x}, \quad s=L\hat{s}, \quad l_t=L\hat{l}, \quad t=L^2\sqrt{\frac{\Lambda_b}{B_b}}\hat{t}, \quad v=\frac{1}{L}\sqrt{\frac{B_b}{\Lambda_b}}\hat{v}, \quad g=\frac{B_b h}{\Lambda_b L^4}\hat{g}, \quad q=\frac{B_b h}{L^4}\hat{q}=\frac{B_b h}{L^4}\Lambda\hat{g} \\ w=\hat{w}h, \quad w_h=\hat{w}_h h, \quad w_f=\hat{w}_f h, \quad \varphi=\frac{h}{L}\hat{\varphi}, \quad \varphi_h=\frac{h}{L}\hat{\varphi}_h, \quad \varphi_f=\frac{h}{L}\hat{\varphi}_f \\ M=\frac{B_b h}{L^2}\hat{M}, \quad M_h=\frac{B_b h}{L^2}\hat{M}_h, \quad M_f=\frac{B_b h}{L^2}\hat{M}_f, \quad Q=\frac{B_b h}{L^3}\hat{Q}, \quad Q_h=\frac{B_b h}{L^3}\hat{Q}_h, \quad Q_f=\frac{B_b h}{L^3}\hat{Q}_f \end{aligned} \quad (15)$$

where a superimposed hat is used to denote dimensionless entities. The deflection is scaled with a characteristic thickness h , and two ratios are introduced: the bending ratio $B = B_t / B_b$ and the mass ratio $\Lambda = \Lambda_t / \Lambda_b$. With these dimensionless parameters, the derivatives of the deflection become

$$\begin{aligned} \frac{\partial w(x, t)}{\partial x} &= \frac{h}{L} \frac{\partial \hat{w}}{\partial \hat{x}}, \quad \frac{\partial^2 w(x, t)}{\partial x^2} = \frac{h}{L^2} \frac{\partial^2 \hat{w}}{\partial \hat{x}^2}, \quad \frac{\partial^4 w(x, t)}{\partial x^4} = \frac{h}{L^4} \frac{\partial^4 \hat{w}}{\partial \hat{x}^4} \\ \frac{\partial w(x, t)}{\partial t} &= \frac{h}{L^2} \sqrt{\frac{B_b}{\Lambda_b}} \frac{\partial \hat{w}}{\partial \hat{t}}, \quad \frac{\partial^2 w(x, t)}{\partial t^2} = \frac{h}{L^4} \frac{B_b}{\Lambda_b} \frac{\partial^2 \hat{w}}{\partial \hat{t}^2} \\ \frac{\partial^2 w(x, t)}{\partial x \partial t} &= \frac{h}{L^3} \sqrt{\frac{B_b}{\Lambda_b}} \frac{\partial^2 \hat{w}}{\partial \hat{x} \partial \hat{t}} \end{aligned} \quad (16)$$

Now the differential equation Eqs. given in Eqs. (4) and (8) and the BCs from Eq. (10) to Eq. (14) can be written, using the formulations from Eqs. (15) - (16), in a dimensionless form as:

- for the loaded part of the bridge

$$(1+B) \frac{\partial^4 \hat{w}(\hat{x}, \hat{t})}{\partial \hat{x}^4} + (1+\Lambda) \frac{\partial^2 \hat{w}(\hat{x}, \hat{t})}{\partial \hat{t}^2} + \Lambda \left[2\dot{\hat{s}} \frac{\partial^2 \hat{w}(\hat{x}, \hat{t})}{\partial \hat{x} \partial \hat{t}} + (\dot{\hat{s}})^2 \frac{\partial^2 \hat{w}(\hat{x}, \hat{t})}{\partial \hat{x}^2} \right] = \Lambda \hat{g} \quad (17)$$

- for the unloaded part of the bridge

$$\frac{\partial^4 \hat{w}(\hat{x}, \hat{t})}{\partial \hat{x}^4} + \frac{\partial^2 \hat{w}(\hat{x}, \hat{t})}{\partial \hat{t}^2} = 0 \quad (18)$$

The BC at the both ends of the bridge are:

- for the **LC1** : $\widehat{w}(0, \widehat{t}) = \widehat{w}_f(\widehat{L}, \widehat{t}) = 0$

$$\widehat{M}(0, \widehat{t}) = -(1+B) \frac{\partial^2 \widehat{w}(0, \widehat{t})}{\partial \widehat{x}^2} = \widehat{M}_0^t, \quad \widehat{M}_f(\widehat{L}, \widehat{t}) = -\frac{\partial^2 \widehat{w}_f(\widehat{L}, \widehat{t})}{\partial \widehat{x}^2} = 0 \quad (19)$$

- for the **LC2** : $\widehat{w}_h(0, \widehat{t}) = \widehat{w}_f(\widehat{L}, \widehat{t}) = 0$ (20)

$$\widehat{M}_h(0, \widehat{t}) = \widehat{M}_f(\widehat{L}, \widehat{t}) = 0$$

- for the **LC3** : $\widehat{w}_h(0, \widehat{t}) = \widehat{w}(\widehat{L}, \widehat{t}) = 0$

$$\widehat{M}_h(0, \widehat{t}) = -\frac{\partial^2 \widehat{w}_h(0, \widehat{t})}{\partial \widehat{x}^2} = 0, \quad \widehat{M}(\widehat{L}, \widehat{t}) = -(1+B) \frac{\partial^2 \widehat{w}(\widehat{L}, \widehat{t})}{\partial \widehat{x}^2} = \widehat{M}_L^t \quad (21)$$

The BC for the end of the train are

$$\begin{aligned} \widehat{M}_h(\widehat{s} - \widehat{l}, \widehat{t}) &= -\frac{\partial^2 \widehat{w}_h(\widehat{s} - \widehat{l}, \widehat{t})}{\partial \widehat{x}^2} = \widehat{M}_{s-l}, \quad \widehat{Q}_h(\widehat{s} - \widehat{l}, \widehat{t}) = -\frac{\partial^3 \widehat{w}_h(\widehat{s} - \widehat{l}, \widehat{t})}{\partial \widehat{x}^3} = \widehat{Q}_{s-l} \\ \widehat{M}(\widehat{s} - \widehat{l}, \widehat{t}) &= -(1+B) \frac{\partial^2 \widehat{w}(\widehat{s} - \widehat{l}, \widehat{t})}{\partial \widehat{x}^2} = \widehat{M}_{s-l}, \quad \widehat{Q}(\widehat{s} - \widehat{l}, \widehat{t}) = -(1+B) \frac{\partial^3 \widehat{w}(\widehat{s} - \widehat{l}, \widehat{t})}{\partial \widehat{x}^3} = \widehat{Q}_{s-l} \end{aligned} \quad (22)$$

The BC for the front of the train are

$$\begin{aligned} \widehat{M}(\widehat{s}, \widehat{t}) &= -(1+B) \frac{\partial^2 \widehat{w}(\widehat{s}, \widehat{t})}{\partial \widehat{x}^2} = \widehat{M}_s, \quad \widehat{Q}(\widehat{s}, \widehat{t}) = -(1+B) \frac{\partial^3 \widehat{w}(\widehat{s}, \widehat{t})}{\partial \widehat{x}^3} = \widehat{Q}_s \\ \widehat{M}_f(\widehat{s}, \widehat{t}) &= -\frac{\partial^2 \widehat{w}_f(\widehat{s}, \widehat{t})}{\partial \widehat{x}^2} = \widehat{M}_s, \quad \widehat{Q}_f(\widehat{s}, \widehat{t}) = -\frac{\partial^3 \widehat{w}_f(\widehat{s}, \widehat{t})}{\partial \widehat{x}^3} = \widehat{Q}_s \end{aligned} \quad (23)$$

The continuity conditions from (14) reads in a non-dimensional form as

$$\begin{aligned} \widehat{w}_h(\widehat{x} = \widehat{s} - \widehat{l}) &= \widehat{w}(\widehat{x} = \widehat{s} - \widehat{l}), \quad \widehat{\varphi}_h(\widehat{x} = \widehat{s} - \widehat{l}) = \widehat{\varphi}(\widehat{x} = \widehat{s} - \widehat{l}) \\ \widehat{w}(\widehat{x} = \widehat{s}) &= \widehat{w}_f(\widehat{x} = \widehat{s}), \quad \widehat{\varphi}(\widehat{x} = \widehat{s}) = \widehat{\varphi}_f(\widehat{x} = \widehat{s}) \end{aligned} \quad (24)$$

In a first step, only the dynamic response of the bridge due to the part of the train that travels on the bridge is interested in, so it is assumed that $\widehat{M}_0^t = \widehat{M}_L^t = 0$ and $\widehat{Q}_0^t = \widehat{Q}_L^t = 0$. In this way, the computational effort could also be keep low.

3. Solution by means of symbolic computation

The differential equations presented in Section 2 were solved by means of symbolic computations. In the domain of small deformation, which implies linearity of the solution, the deflection of the system is split into two parts, namely a (quasi-) static and a dynamic part

$$\widehat{w} = \widehat{w}^s + \widehat{w}^d \tag{25}$$

where the superscripts *s* and *d* are used to denote the static and dynamic part, respectively. The advantage of this splitting is a better convergence of the series solutions to be introduced. According to Eq. (25), Eqs. (17) and (18) can be re-written as:

- the loaded part of the bridge

- the static part: $(1+B) \frac{\partial^4 \widehat{w}^s(\widehat{x}, \widehat{t})}{\partial \widehat{x}^4} = \Lambda \widehat{g}$ (26)

- the dynamic part:

$$\begin{aligned} & (1+B) \frac{\partial^4 \widehat{w}^d(\widehat{x}, \widehat{t})}{\partial \widehat{x}^4} + (1+\Lambda) \frac{\partial^2 \widehat{w}^d(\widehat{x}, \widehat{t})}{\partial \widehat{t}^2} + \Lambda \left[2\dot{\widehat{s}} \frac{\partial^2 \widehat{w}^d(\widehat{x}, \widehat{t})}{\partial \widehat{x} \partial \widehat{t}} + (\dot{\widehat{s}})^2 \frac{\partial^2 \widehat{w}^d(\widehat{x}, \widehat{t})}{\partial \widehat{x}^2} \right] + \\ & + (1+\Lambda) \frac{\partial^2 \widehat{w}^s(\widehat{x}, \widehat{t})}{\partial \widehat{t}^2} + \Lambda \left[2\dot{\widehat{s}} \frac{\partial^2 \widehat{w}^s(\widehat{x}, \widehat{t})}{\partial \widehat{x} \partial \widehat{t}} + (\dot{\widehat{s}})^2 \frac{\partial^2 \widehat{w}^s(\widehat{x}, \widehat{t})}{\partial \widehat{x}^2} \right] = 0 \end{aligned} \tag{27}$$

- the unloaded part of the bridge

- the static part: $\frac{\partial^4 \widehat{w}_{h,f}^s(\widehat{x}, \widehat{t})}{\partial \widehat{x}^4} = 0$ (28)

- the dynamic part: $\frac{\partial^4 \widehat{w}_{h,f}^d(\widehat{x}, \widehat{t})}{\partial \widehat{x}^4} + \frac{\partial^2 \widehat{w}_{h,f}^d(\widehat{x}, \widehat{t})}{\partial \widehat{t}^2} + \frac{\partial^2 \widehat{w}_{h,f}^s(\widehat{x}, \widehat{t})}{\partial \widehat{t}^2} = 0$ (29)

To simplify the equations, the terms in Eq. (27) containing the static displacement by *LSP* is denoted as

$$LSP = (1+\Lambda) \frac{\partial^2 \widehat{w}^s(\widehat{x}, \widehat{t})}{\partial \widehat{t}^2} + \Lambda \left[2\dot{\widehat{s}} \frac{\partial^2 \widehat{w}^s(\widehat{x}, \widehat{t})}{\partial \widehat{x} \partial \widehat{t}} + (\dot{\widehat{s}})^2 \frac{\partial^2 \widehat{w}^s(\widehat{x}, \widehat{t})}{\partial \widehat{x}^2} \right] \tag{30}$$

and the static contribution in Eq. (29) as *HSP* for the unloaded part of the bridge behind the train and *FSP* for the unloaded part of the bridge in front of the train

$$HSP = \frac{\partial^2 \widehat{w}_h^s(\widehat{x}, \widehat{t})}{\partial \widehat{t}^2}, \quad FSP = \frac{\partial^2 \widehat{w}_f^s(\widehat{x}, \widehat{t})}{\partial \widehat{t}^2} \tag{31}$$

The BCs from Eqs. (19) to (23) are also split into a static part and a dynamic part, as well as the continuity conditions from Eq. (24) at the locations $\hat{x}=\hat{s}-\hat{l}$ and $\hat{x}=\hat{s}$. For this strategy see also (Cojocaru *et al.* 2004).

3.1 The static solution

For the static solution, the Laplace transformation method is used, carried out with respect to x

$$\bar{W}(\omega, \hat{t}) = L[\hat{w}(\hat{x}, \hat{t})] = \int_0^{\infty} \hat{w}(\hat{x}, \hat{t}) e^{-\omega \hat{x}} d\omega \quad (32)$$

where w is the complex variable of Laplace transform. Taking the Laplace transform of Eqs. (26) and (28), and considering the static part of the BC from Eqs. (19) to (23), for each loading case, an equation of deflection is obtained for the unloaded and loaded part of the bridge. The unknowns will be determinate from BCs, from transition conditions and from the continuity conditions at the locations $\hat{x}=\hat{s}-\hat{l}$ and $\hat{x}=\hat{s}$, (Cojocaru *et al.* 2004). Taking into account that $\hat{L}=1$, the expressions of static deflection of the system “bridge-train” become:

- for the **LC1**:

- the loaded part of the bridge

$$w = \frac{\Lambda \hat{g} \hat{x}^3}{24(1+B)} (\hat{x} + 2\hat{s}^2 - 4\hat{s}) - \frac{\Lambda \hat{g} \hat{x}^3}{8(1+B)} (B\hat{s}^5 - 3\hat{s}^4 B + 3\hat{s}^3 B - B\hat{s}^2 + \hat{s}^3 - \hat{s}^4 - \hat{s}^2) \quad (33)$$

- the unloaded part of the bridge in front of the train

$$w_f = \frac{\Lambda \hat{g} \hat{s}^2 (\hat{x}-1)}{24(1+B)} (2\hat{x}^2 B + 2\hat{x}^2 - 4\hat{x} B - 4\hat{x} - 4\hat{s}^3 B + 6\hat{s}^2 B + \hat{s}^2) \quad (34)$$

- for the **LC2**:

- the unloaded part of the bridge behind of the train

$$\begin{aligned} w_h = & \frac{\Lambda \hat{g} \hat{l} \hat{x}^3}{12(1+B)} (2\hat{s} B + 2\hat{s} - \hat{l} - 2B - 2) + \frac{\Lambda \hat{g} \hat{s} \hat{l}^2 B \hat{x}}{12(1+B)} (-12\hat{s}^2 + 18\hat{s} \hat{l} + 21\hat{s} - 24\hat{l} - 10\hat{l}^2 - 6) + \\ & + \frac{\Lambda \hat{g} \hat{s} \hat{l}^2 \hat{x}}{12(1+B)} (-3\hat{s} + 2\hat{l} + 6) + \frac{\Lambda \hat{g} \hat{l} \hat{s} \hat{x}}{12(1+B)} (2\hat{s}^2 B - 6\hat{s} B + 4B + 2\hat{s}^2 - 6\hat{s} + 4) + \\ & + \frac{\Lambda \hat{g} \hat{l} \hat{x}}{24(1+B)} (14\hat{l}^3 B + 12\hat{l}^2 B - 4\hat{l} B + 4\hat{l}^4 B - \hat{l}^3 - 4\hat{l}^2 - 4\hat{l}) \end{aligned} \quad (35)$$

- the loaded part of the bridge

$$\begin{aligned}
 w = & \frac{\Lambda \widehat{g} \widehat{x}^3}{24(1+B)} \left(-2\widehat{l}^2 + 4\widehat{l}\widehat{s} - 4\widehat{s} \right) + \frac{\Lambda \widehat{g} \widehat{x}^2}{24(1+B)} \left(6\widehat{l}^2 - 12\widehat{l}\widehat{s} + 6\widehat{s}^2 \right) + \\
 & + \frac{\Lambda \widehat{g} \widehat{x}}{24(1+B)} \left(4\widehat{l}^5 B - 20\widehat{l}^4 \widehat{s} B + 8\widehat{l}^4 B - \widehat{l}^4 + 36\widehat{l}^3 \widehat{s}^2 B - 24\widehat{l}^3 \widehat{s} B + 4\widehat{l}^3 \widehat{s} - 24\widehat{l}^2 \widehat{s}^3 B + 12\widehat{l}^2 \widehat{s}^2 B + \right. \\
 & + 12\widehat{l}^2 \widehat{s} B - 6\widehat{l}^2 \widehat{s}^2 - 4\widehat{l}^2 + 16\widehat{l} \widehat{s}^3 B - 24\widehat{l} \widehat{s}^2 B + 8\widehat{l} \widehat{s} B + 8\widehat{l} \widehat{s} - 4\widehat{l}^2 B - 4\widehat{s}^3 \left. \right) + \\
 & + \frac{\Lambda \widehat{g}}{24(1+B)} \left(-4\widehat{l}^5 B + 20\widehat{l}^4 \widehat{s} B - 8\widehat{l}^4 B + \widehat{l}^4 - 36\widehat{l}^3 \widehat{s}^2 B - 4\widehat{l}^3 \widehat{s} - 24\widehat{l}^2 \widehat{s}^2 B + 6\widehat{l}^2 \widehat{s}^2 + 8\widehat{l} \widehat{s}^3 B - 4\widehat{l} \widehat{s}^3 + \widehat{s}^4 \right)
 \end{aligned} \tag{36}$$

- the unloaded part of the bridge in front of the train

$$\begin{aligned}
 w_f = & \frac{\Lambda \widehat{g} \widehat{l} \widehat{x}^2 (\widehat{x}-1)}{12(1+B)} \left(2\widehat{s} B - \widehat{l} - B\widehat{l} + 2\widehat{s} \right) + \frac{\Lambda \widehat{g} \widehat{l} \widehat{x} (\widehat{x}-1)}{12(1+B)} \left(2\widehat{l} B - 4\widehat{s} B - 4\widehat{s} + 2\widehat{l} \right) \\
 & + \frac{\Lambda \widehat{g} \widehat{l} (\widehat{x}-1)}{24(1+B)} \left(4\widehat{l}^4 B - 20\widehat{l}^3 \widehat{s} B + 8\widehat{l}^3 B - \widehat{l}^3 + 36\widehat{l}^2 \widehat{s}^2 B - 24\widehat{l}^2 \widehat{s} B + 4\widehat{l}^2 \widehat{s} - 24\widehat{l} \widehat{s}^3 B + 4\widehat{s}^3 \right. \\
 & \left. + 18\widehat{l} \widehat{s}^2 B - 6\widehat{l} \widehat{s}^2 + 4\widehat{s}^3 B \right)
 \end{aligned} \tag{37}$$

- for the LC3:

- the unloaded part of the bridge behind the train

$$\begin{aligned}
 w_h = & \frac{\Lambda \widehat{g} \widehat{x}^3}{12(1+B)} \left(-\widehat{l}^2 B - \widehat{l}^2 + 2\widehat{l} \widehat{s} B + 2\widehat{l} \widehat{s} - 2B\widehat{l} - 2\widehat{l} - \widehat{s}^2 B - \widehat{s}^2 + 2\widehat{s} B + 2\widehat{s} - B - 1 \right) \\
 & + \frac{\Lambda \widehat{g} \widehat{x}}{24(1+B)} \left(-4\widehat{s}^5 B + 20\widehat{s}^4 \widehat{l} B + 14\widehat{s}^4 B - \widehat{s}^4 - 40\widehat{s}^3 \widehat{l}^2 B - 56\widehat{s}^3 \widehat{l} B - 16\widehat{s}^3 B + 4\widehat{s}^3 \widehat{l} + 4\widehat{s}^3 \right. \\
 & + 40\widehat{s}^2 \widehat{l}^3 B + 84\widehat{s}^2 \widehat{l}^2 B + 48\widehat{s}^2 \widehat{l} B - 6\widehat{s}^2 \widehat{l}^2 - 12\widehat{s}^2 \widehat{l} + 6\widehat{s}^2 B - 4\widehat{s}^2 - 56\widehat{s} \widehat{l}^3 B - 48\widehat{s} \widehat{l}^2 B - 12\widehat{s} \widehat{l} B \\
 & \left. + 8\widehat{s} \widehat{l} + 4\widehat{s} \widehat{l}^3 - 20\widehat{s} \widehat{l}^4 + 4\widehat{l}^5 B + 14\widehat{l}^4 B - \widehat{l}^4 + 16\widehat{l}^3 B - 4\widehat{l}^3 + 6\widehat{l}^2 B - 4\widehat{l}^2 \right)
 \end{aligned} \tag{38}$$

- the loaded part of the bridge

$$\begin{aligned}
 w = & \frac{\Lambda \widehat{g} \widehat{x}^3 (\widehat{x}-1)}{24(1+B)} + \frac{\Lambda \widehat{g} \widehat{x}^2 (\widehat{x}-1)}{24(1+B)} \left(-2\widehat{s}^2 + 4\widehat{s} \widehat{l} - 2\widehat{l}^2 - 1 \right) + \frac{\Lambda \widehat{g} \widehat{x} (\widehat{x}-1)}{24(1+B)} \left(4\widehat{s}^2 - 8\widehat{s} \widehat{l} + 4\widehat{l}^2 - 1 \right) \\
 & + \left(20\widehat{s}^4 \widehat{l} + 8\widehat{s}^4 B - \widehat{s}^4 - 40\widehat{s}^3 \widehat{l}^2 B - 32\widehat{s}^3 \widehat{l} B + 4\widehat{s}^3 \widehat{l} - 4\widehat{s}^3 B + 40\widehat{s}^2 \widehat{l}^3 B + 48\widehat{s}^2 \widehat{l}^2 B + 12\widehat{s}^3 \widehat{l} B - 6\widehat{s}^2 \widehat{l}^2 \right. \\
 & \left. - 20\widehat{s} \widehat{l}^4 B - 32\widehat{s} \widehat{l}^3 B - 12\widehat{s} \widehat{l}^2 B + 4\widehat{s} \widehat{l}^3 + 4\widehat{l}^5 B + 8\widehat{l}^4 B - \widehat{l}^4 + 4\widehat{l}^3 B \right)
 \end{aligned} \tag{39}$$

3.2 The dynamic solution

The next step is to solve the differential equations from Eqs. (27) and (29) to obtain the dynamic solution. For this scope, a Ritz - Galerkin procedure is used, where the dynamic deflection is assumed in the form of a finite series of functions separable in space and time, (Ziegler 1991).

$$\widehat{w}^{d,*}(\widehat{x},\widehat{t}) = \sum_{j=1}^n \widehat{p}_j(\widehat{t})\widehat{\Phi}_j(\widehat{x}), \text{ with } \widehat{\Phi}_j(\widehat{x}) = \sin \frac{j\pi\widehat{x}}{\widehat{L}} \quad (40)$$

where $\widehat{p}_j(\widehat{t})$ are the n generalised co-ordinates, and $\widehat{\Phi}_j(\widehat{x})$ are the modes of natural vibrations of a simply supported homogeneous beam. When substitute the approximate solution (40) into the governing Eqs. (27) and (29), and apply the Galerkin procedure with the virtual variation of the assumed solution as

$$\delta\widehat{w}^{d,*}(\widehat{x},\widehat{t}) = \sum_{j=1}^n \delta\widehat{p}_j(\widehat{t})\widehat{\Phi}_j(\widehat{x}) \quad (41)$$

and after some mathematical manipulations, an expression is obtained as the form

- for the **LC1**:

$$\begin{aligned} & \int_0^{\widehat{s}} \widehat{\Phi}_i(\widehat{x}) \left[(1+B) \sum_{j=1}^n \widehat{p}_j \widehat{\Phi}_j''''(\widehat{x}) + (1+\Lambda) \sum_{j=1}^n \ddot{\widehat{p}}_j \widehat{\Phi}_j(\widehat{x}) \right] d\widehat{x} + \int_0^{\widehat{s}} \widehat{\Phi}_i(\widehat{x}) \left[2\dot{\widehat{s}} \sum_{j=1}^n \dot{\widehat{p}}_j \widehat{\Phi}_j'(\widehat{x}) \right. \\ & \left. + (\dot{\widehat{s}})^2 \sum_{j=1}^n \widehat{p}_j \widehat{\Phi}_j(\widehat{x}) \right] d\widehat{x} + \int_0^{\widehat{s}} \widehat{\Phi}_i(\widehat{x}) LSP d\widehat{x} + \int_{\widehat{s}}^{\widehat{L}} \widehat{\Phi}_i(\widehat{x}) \left[\sum_{j=1}^n \widehat{p}_j \widehat{\Phi}_j''''(\widehat{x}) + \sum_{j=1}^n \ddot{\widehat{p}}_j \widehat{\Phi}_j(\widehat{x}) + FSP \right] d\widehat{x} = 0 \end{aligned} \quad (42)$$

- for the **LC2**:

$$\begin{aligned} & \int_0^{\widehat{s}-\widehat{l}} \widehat{\Phi}_i(\widehat{x}) \left[\sum_{j=1}^n \widehat{p}_j \widehat{\Phi}_j''''(\widehat{x}) + \sum_{j=1}^n \ddot{\widehat{p}}_j \widehat{\Phi}_j(\widehat{x}) + HSP \right] d\widehat{x} + \int_{\widehat{s}-\widehat{l}}^{\widehat{s}} \widehat{\Phi}_i(\widehat{x}) \left[(1+B) \sum_{j=1}^n \widehat{p}_j \widehat{\Phi}_j''''(\widehat{x}) \right. \\ & \left. + (1+\Lambda) \sum_{j=1}^n \ddot{\widehat{p}}_j \widehat{\Phi}_j(\widehat{x}) \right] d\widehat{x} + \int_{\widehat{s}-\widehat{l}}^{\widehat{s}} \widehat{\Phi}_i(\widehat{x}) \left[2\dot{\widehat{s}} \sum_{j=1}^n \dot{\widehat{p}}_j \widehat{\Phi}_j'(\widehat{x}) + (\dot{\widehat{s}})^2 \sum_{j=1}^n \widehat{p}_j \widehat{\Phi}_j(\widehat{x}) \right] d\widehat{x} + \int_{\widehat{s}-\widehat{l}}^{\widehat{s}} \widehat{\Phi}_i(\widehat{x}) LSP d\widehat{x} \\ & + \int_{\widehat{s}}^{\widehat{L}} \widehat{\Phi}_i(\widehat{x}) \left[\sum_{j=1}^n \widehat{p}_j \widehat{\Phi}_j''''(\widehat{x}) + \sum_{j=1}^n \ddot{\widehat{p}}_j \widehat{\Phi}_j(\widehat{x}) + FSP \right] d\widehat{x} = 0 \end{aligned} \quad (43)$$

- for the **LC3**:

$$\begin{aligned}
 & \int_0^{\hat{s}-\hat{l}} \hat{\Phi}_i(\hat{x}) \left[\sum_{j=1}^n \hat{p}_j \hat{\Phi}_j'''(\hat{x}) + \sum_{j=1}^n \ddot{\hat{p}}_j \hat{\Phi}_j(\hat{x}) + HSP \right] d\hat{x} \\
 & + \int_{\hat{s}-\hat{l}}^{\hat{L}} \hat{\Phi}_i(\hat{x}) \left[(1+B) \sum_{j=1}^n \hat{p}_j \hat{\Phi}_j'''(\hat{x}) + (1+\Lambda) \sum_{j=1}^n \ddot{\hat{p}}_j \hat{\Phi}_j(\hat{x}) \right] d\hat{x} \\
 & + \int_{\hat{s}-\hat{l}}^{\hat{L}} \hat{\Phi}_i(\hat{x}) \left[2\dot{\hat{s}} \sum_{j=1}^n \dot{\hat{p}}_j \hat{\Phi}_j'(\hat{x}) + (\dot{\hat{s}})^2 \right] \sum_{j=1}^n \hat{p}_j \hat{\Phi}_j(\hat{x}) \Bigg] + \int_{\hat{s}-\hat{l}}^{\hat{L}} \hat{\Phi}_i(\hat{x}) LSP d\hat{x} = 0
 \end{aligned} \quad (44)$$

After re-arrange the Eqs. (42), (43) and (44) collecting for the derivatives of the generalized coordinates, they can be put into a matrix form as follows

$$\mathbf{M}_{1,2,3} \ddot{\mathbf{p}} + \mathbf{C}_{1,2,3} \dot{\mathbf{p}} + \mathbf{K}_{1,2,3} \mathbf{p} + \mathbf{f}_{1,2,3} = 0 \quad (45)$$

where the indices 1,2,3 refer to the load case. The coefficients from Eq. (45) are matrices with elements of the form

- the mass matrix $\mathbf{M}_{1,2,3} = [m_{ij}^{1,2,3}]$ with $i, j = 1, 2, \dots, n$, is a $n \times n$ matrix

$$\begin{aligned}
 \mathbf{LC1}: m_{ij}^1 &= (1+\Lambda) \int_0^{\hat{s}} \hat{\Phi}_i(\hat{x}) \hat{\Phi}_j(\hat{x}) d\hat{x} + \int_{\hat{s}}^{\hat{L}} \hat{\Phi}_i(\hat{x}) \hat{\Phi}_j(\hat{x}) d\hat{x} \\
 \mathbf{LC2}: m_{ij}^2 &= \int_0^{\hat{s}-\hat{l}} \hat{\Phi}_i(\hat{x}) \hat{\Phi}_j(\hat{x}) d\hat{x} + (1+\Lambda) \int_{\hat{s}-\hat{l}}^{\hat{s}} \hat{\Phi}_i(\hat{x}) \hat{\Phi}_j(\hat{x}) d\hat{x} + \int_{\hat{s}}^{\hat{L}} \hat{\Phi}_i(\hat{x}) \hat{\Phi}_j(\hat{x}) d\hat{x} \\
 \mathbf{LC3}: m_{ij}^3 &= \int_0^{\hat{s}-\hat{l}} \hat{\Phi}_i(\hat{x}) \hat{\Phi}_j(\hat{x}) d\hat{x} + (1+\Lambda) \int_{\hat{s}-\hat{l}}^{\hat{L}} \hat{\Phi}_i(\hat{x}) \hat{\Phi}_j(\hat{x}) d\hat{x}
 \end{aligned} \quad (46)$$

- the damping matrix $\mathbf{C}_{1,2,3} = [c_{ij}^{1,2,3}]$ with $i, j = 1, 2, \dots, n$, is a $n \times n$ matrix

$$\begin{aligned}
 \mathbf{LC1}: c_{ij}^1 &= (2\dot{\hat{s}}\Lambda) \int_0^{\hat{s}} \hat{\Phi}_i(\hat{x}) \hat{\Phi}_j'(\hat{x}) d\hat{x}, \quad \mathbf{LC2}: c_{ij}^2 = (2\dot{\hat{s}}\Lambda) \int_{\hat{s}-\hat{l}}^{\hat{s}} \hat{\Phi}_i(\hat{x}) \hat{\Phi}_j'(\hat{x}) d\hat{x} \\
 \mathbf{LC3}: c_{ij}^3 &= (2\dot{\hat{s}}\Lambda) \int_{\hat{s}-\hat{l}}^{\hat{L}} \hat{\Phi}_i(\hat{x}) \hat{\Phi}_j'(\hat{x}) d\hat{x}
 \end{aligned} \quad (47)$$

- the stiffness matrix $\mathbf{K}_{1,2,3} = [k_{ij}^{1,2,3}]$ with $i, j = 1, 2, \dots, n$, is a $n \times n$ matrix

$$\begin{aligned}
 \text{LC1: } k_{ij}^1 &= (1+B) \int_0^{\hat{s}} \hat{\Phi}_i(\hat{x}) \hat{\Phi}_j''''(\hat{x}) d\hat{x} + (\hat{s})^2 \int_0^{\hat{s}} \hat{\Phi}_i(\hat{x}) \hat{\Phi}_j''(\hat{x}) d\hat{x} + \int_{\hat{s}}^{\hat{L}} \hat{\Phi}_i(\hat{x}) \hat{\Phi}_j''''(\hat{x}) d\hat{x} \\
 \text{LC2: } k_{ij}^2 &= \int_0^{\hat{s}-\hat{l}} \hat{\Phi}_i(\hat{x}) \hat{\Phi}_j''''(\hat{x}) d\hat{x} + (1+B) \int_{\hat{s}-\hat{l}}^{\hat{s}} \hat{\Phi}_i(\hat{x}) \hat{\Phi}_j''''(\hat{x}) d\hat{x} + (\hat{s})^2 \int_{\hat{s}-\hat{l}}^{\hat{s}} \hat{\Phi}_i(\hat{x}) \hat{\Phi}_j''(\hat{x}) d\hat{x} \\
 &\quad + \int_{\hat{s}}^{\hat{L}} \hat{\Phi}_i(\hat{x}) \hat{\Phi}_j''''(\hat{x}) d\hat{x} \\
 \text{LC3: } k_{ij}^3 &= \int_0^{\hat{s}-\hat{l}} \hat{\Phi}_i(\hat{x}) \hat{\Phi}_j''''(\hat{x}) d\hat{x} + (1+B) \int_{\hat{s}-\hat{l}}^{\hat{L}} \hat{\Phi}_i(\hat{x}) \hat{\Phi}_j''''(\hat{x}) d\hat{x} + (\hat{s})^2 \int_{\hat{s}-\hat{l}}^{\hat{L}} \hat{\Phi}_i(\hat{x}) \hat{\Phi}_j''(\hat{x}) d\hat{x}
 \end{aligned} \tag{48}$$

- the vectors of external loads $\mathbf{f}_{1,2,3} = [f_i^{1,2,3}]$ with $i = 1, 2, \dots, n$, is a $n \times n$ matrix

$$\begin{aligned}
 \text{LC1: } f_i^1 &= \int_0^{\hat{s}} \hat{\Phi}_i(\hat{x}) LSP d\hat{x} + \int_{\hat{s}}^{\hat{L}} \hat{\Phi}_i(\hat{x}) FSP d\hat{x} \\
 \text{LC2: } f_i^2 &= \int_0^{\hat{s}-\hat{l}} \hat{\Phi}_i(\hat{x}) HSP d\hat{x} + \int_{\hat{s}-\hat{l}}^{\hat{s}} \hat{\Phi}_i(\hat{x}) LSP d\hat{x} + \int_{\hat{s}}^{\hat{L}} \hat{\Phi}_i(\hat{x}) FSP d\hat{x} \\
 \text{LC3: } f_i^2 &= \int_0^{\hat{s}-\hat{l}} \hat{\Phi}_i(\hat{x}) HSP d\hat{x} + \int_{\hat{s}-\hat{l}}^{\hat{L}} \hat{\Phi}_i(\hat{x}) LSP d\hat{x}
 \end{aligned} \tag{49}$$

In order to obtain the solutions of the problem under consideration, the systems of differential equations second order from Eq. (45) were transformed into a system of differential equations of first order

$$\dot{\mathbf{X}} = \mathbf{A}\mathbf{X} + \mathbf{b} \tag{50}$$

where

$$\text{- } \mathbf{X} \text{ denotes the state vector of the form: } \mathbf{X}^T = [\mathbf{p} \quad \dot{\mathbf{p}}] \tag{51}$$

$$\text{- } \mathbf{A} \text{ is the coefficients matrix of the form: } \mathbf{A} = \begin{bmatrix} \mathbf{0} & \mathbf{E} \\ -\mathbf{M}^{-1}\mathbf{K} & -\mathbf{M}^{-1}\mathbf{C} \end{bmatrix} \tag{52}$$

$$\text{- } \mathbf{b} \text{ is the vector of external loads of the form: } \mathbf{b}^T = [\mathbf{0} \quad -\mathbf{M}^{-1}\mathbf{f}] \tag{53}$$

Hence, the first order differential equations can be written in the extend form

$$\begin{bmatrix} \dot{\mathbf{p}} \\ \ddot{\mathbf{p}} \end{bmatrix} = \begin{bmatrix} \mathbf{0} & \mathbf{E} \\ -\mathbf{M}^{-1}\mathbf{K} & -\mathbf{M}^{-1}\mathbf{C} \end{bmatrix} \begin{bmatrix} \mathbf{p} \\ \dot{\mathbf{p}} \end{bmatrix} + \begin{bmatrix} \mathbf{0} \\ -\mathbf{M}^{-1}\mathbf{f} \end{bmatrix} \quad (54)$$

The symbolic computer code *Maple9.5* is used to obtain the static solution of the system, to build the system of differential equations of second order and to transform this into the system of differential equations of first order, taking the time as an additional variable. The solution of this system is obtained through numerical simulations with the help of MatLab/Simulink. A fixed-step continuous solver, that is a fifth order Dormand-Prince formula (MatLab On-line Manual) was used with the fixed-step size of 0.001.

4. Numerical results

In order to illustrate the influence of bending stiffness of the train upon the deflection, bending moment and shear force in the bridge, a series of symbolic computations are performed. An elastic bridge of 100 m span and unit high ($h = 1$ m), with $I_b = 74.65 \text{ m}^4$ and $A_b = 8.64 \text{ m}^2$ is taken as an example structure. The material is steel with Young's modulus $E = 2.1 \times 10^{11} \text{ N/m}^2$, and density of mass $\rho = 7850 \text{ kg/m}^3$. With the above values one obtains $B_b = 1.5676 \times 10^{13} \text{ Nm}^2$ and $\Lambda_b = 67824 \text{ kg/m}$. The length of the train is 30 m. With these values, a non-dimensional gravitational acceleration $\hat{g} = g \frac{\Lambda_b L^3}{B_b} = 0.042$ was computed. If it is necessary to calculate the dynamic response of a structure with another height, h_1 for example, the non-dimensional gravitational acceleration \hat{g} should be multiplied by L/h_1 . The computations were performed for four values of the non-dimensional stiffness ratio $B = 0, 0.5, 1$ and 1.5 , two values of mass ratio $\Lambda = 0.5$ and 1 , and for six values of the non-dimensional velocity of the train $\hat{s} = \hat{v} = 0.055, 0.2, 0.55, 0.64, 1.096$ and 1.57 , which are the correspondent dimensionless values of 30, 110, 300, 350, 600 and 860 km/h. The last velocity 860 km/h, is the velocity with which the train travels across the bridge in 0.42 s, which represents the period of the first mode of vibration of the unloaded bridge. The first velocity corresponds to a quasi-static load of the bridge.

With the above similarity numbers, the dimensionless deflection \hat{w}_b , bending moment \hat{M}_b and shear-force \hat{Q}_b in the mid-span of the simply supported bridge are determined as a function of time. For the dynamic deflection a Ritz approximation with 5 terms is used. The results for \hat{w}_b , \hat{M}_b and \hat{Q}_b are shown in Figs. 3, 4 and 5. In the following representations, both the forced vibrations of the bridge when the train travels over the bridge and the free vibrations of the bridge after the train leaves the bridge are considered.

Figs. 3(a) and 3(b) show the time histories of deflection at the mid-span of the bridge for two values of the mass ratio Λ and each of them for four values of the bending stiffness ratio B . It can be observed that the deflection at the mid-span of the bridge increases with increasing mass ratio but decreases with the increasing bending stiffness ratio. Fig. 3(c) shows the time history of the deflection at the mid-span of the bridge for four non-dimensional velocities of the train. As can be seen the deflection at the mid-span of the bridge increases also with the increasing traveling velocity of the train, however slowly for non-dimensional velocities until 0.55. For non-dimensional velocities greater as 0.55 the deflection of the bridge increases strongly. The amplitudes of the free vibrations of the bridge also increase with increasing mass ration and traveling velocity.

Shown in Figs. 4(a) and 4(b) are the time histories of the bending moment at the mid-span of the

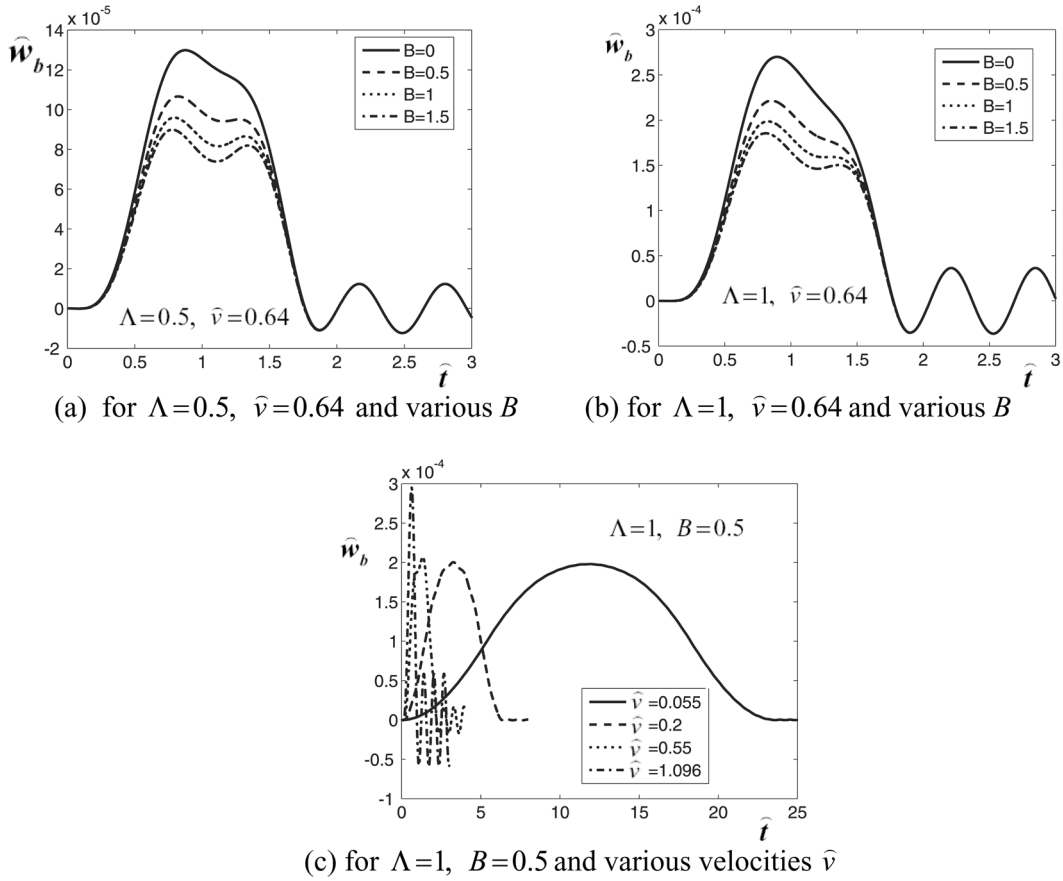


Fig. 3 Deflection \hat{w}_b at the mid-span of the bridge as a function of \hat{t}

bridge for two values of the mass ratio Λ and each of them for four values of the bending stiffness ratio B . As can be seen from Figs. 4, a concentrated moment occurs at the front and the end of the train, which is materialized by the jumps in \hat{M}_b . The jumps occur when the front and the end of the train passes the middle of the bridge. It can be also observed that the bending moment at the mid-span of the bridge increases with mass ratio and decreases with bending stiffness ratio when the train crosses over the middle of the bridge, but the jumps in bending moment increase with stiffness ratio. Fig. 4(c) shows the time history of the bending moment at the mid-span of the bridge for four non-dimensional velocities of the train. The bending moment at the mid-span of the bridge increases with the traveling velocity of the train, and it can be observed the same behavior as by the deflection of the bridge: it increases slowly for non-dimensional velocities until 0.55 and strongly for non-dimensional velocities greater as 0.55. The amplitudes of the free vibrations increase with mass ratio and traveling velocity too.

Shown in Figs. 5(a) and 5(b) are the time histories of shear force at the mid-span of the bridge for two values of the mass ratio Λ and each of them for four values of the bending stiffness ratio B . The shear force at the mid-span of the bridge shows the same behavior towards the mass ratio and bending stiffness ratio as the bending moment. Also in this case concentrated force occurs at the

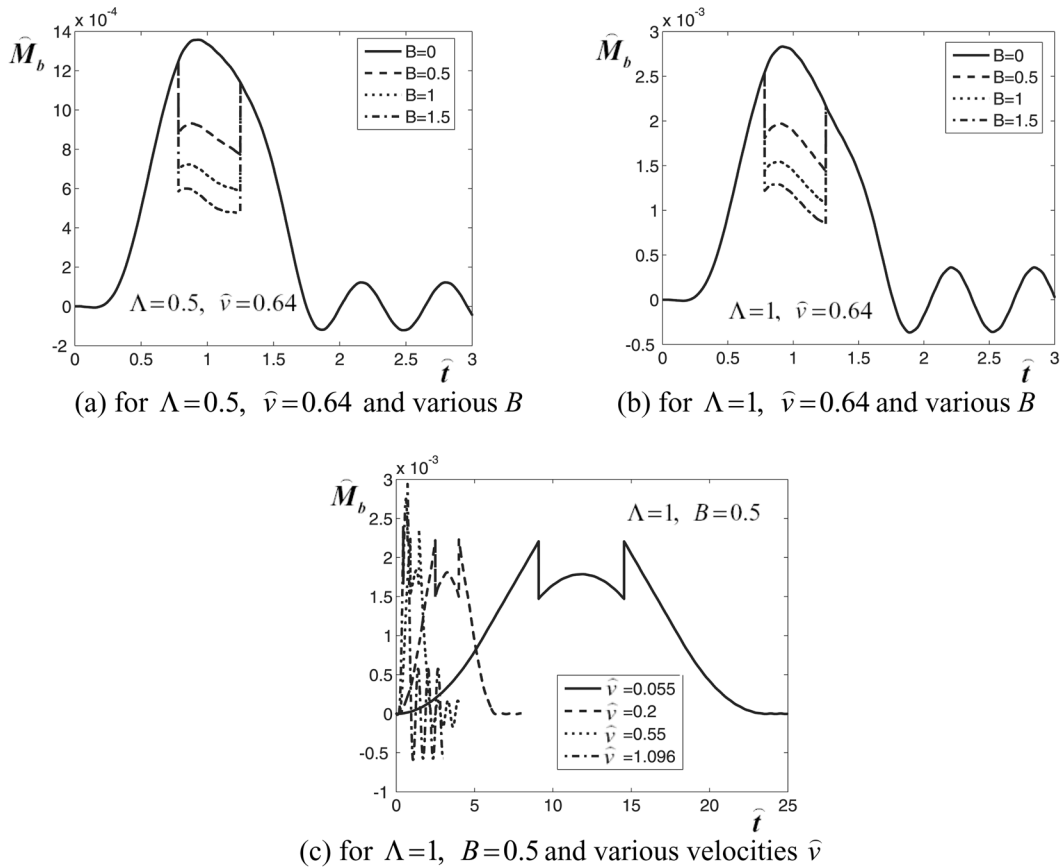


Fig. 4 Deflection \hat{M}_b at the mid-span of the bridge as a function of \hat{t}

front and the end of the train, when these locations pass the middle of the bridge. The concentrated forces are materialized by the jumps in \hat{Q}_b . The jumps occur when the front and the end of the train passes the middle of the bridge, and increase with stiffness ratio. Fig. 5(c) shows the time history of the shear force at the mid-span of the bridge for four non-dimensional velocities of the train. The shear force at the mid-span of the bridge increases with traveling velocity of the train, and it can be observed the same behavior as by the deflection of the bridge: it increases slowly for non-dimensional velocities until 0.55 and a bit strongly for non-dimensional velocities greater as 0.55. The amplitudes of the free vibrations also increase with mass ratio and traveling velocity of the train.

As can be seen from Figs. 4 and 5, a concentrated force and a concentrated moment occur at the front and the end of the train, which are materialized by the jumps in \hat{M}_b and \hat{Q}_b . The jumps occur when the front and the end of the train passes the middle of the bridge, because a rigid interface is assumed between the train and the bridge. This rigid interface imposes that the deflections of the train and the bridge are equal, which implies that the second and third derivative of the deflection of the train do not vanish at this location as shown in Fig. 2(c). In a detailed modeling with a non-rigid interface, the concentrated loads at the front of the train would be represented by pressure concentrations, as shown in (Cojocaru *et al.* 2003).

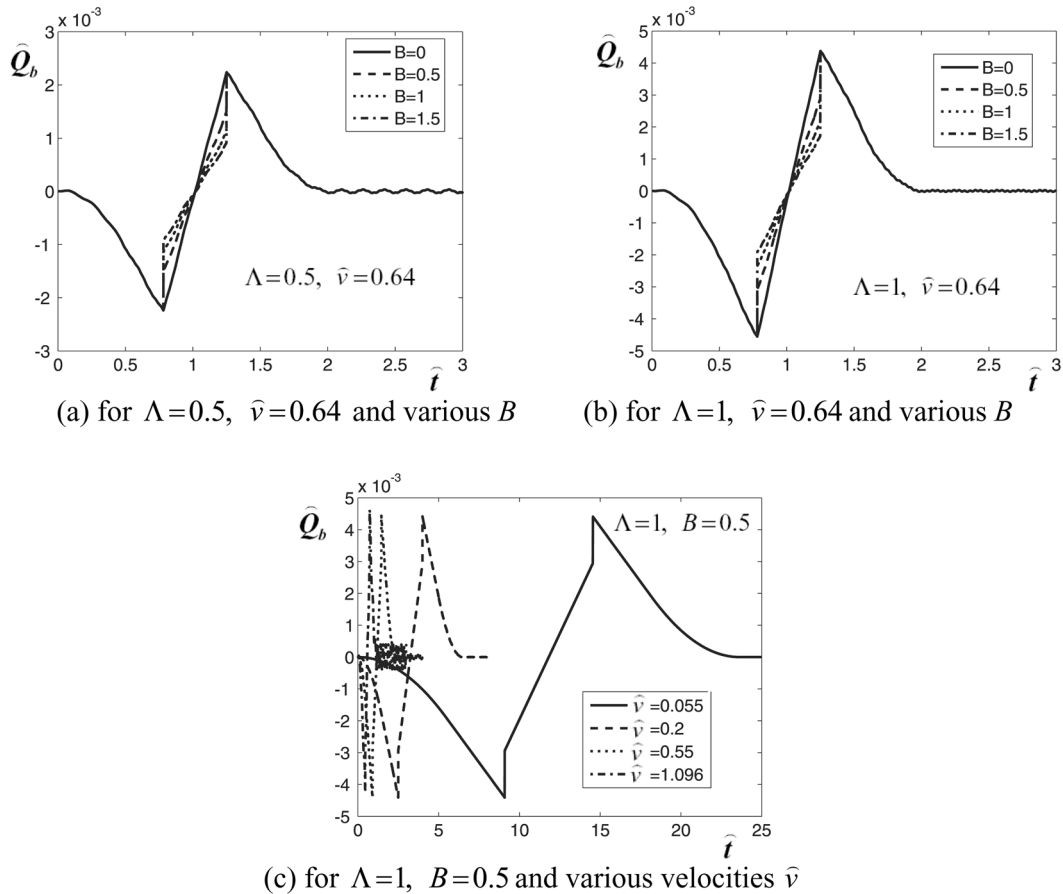


Fig. 5 Shear force \hat{Q}_b at the mid-span of the bridge as a function of \hat{t}

The case of $\hat{v} = 1.57$, i.e. the case in which the train passes the bridge in the period of the first mode of vibration of the unloaded bridge, is treated in comparison with the case of $\hat{v} = 0.64$ in Fig. 6. As can be seen, the passage of the train on the bridge with high velocities, i.e. $\hat{v} = 1.57$ produces considerably high amplitude response of the bridge.

The influence of bending stiffness and mass ratio on the response of the bridge at the mid-span is also investigated for a number of velocities of the train from 0.055 until 1.57 with an increment about 0.1. In this case, the maximum deflection of the bridge is determined for three values of the non-dimensional stiffness ratio, $B = 0.25$, 0.5 and 1, and for three values of the non-dimensional mass ratio, $\Lambda = 0.25$, 0.5 and 1. The results are plotted in Fig. 7. It can be observed that the deflection of the bridge increases slowly for non-dimensional velocities until 0.7 and has a kink at 0.7; and for values of the non-dimensional velocity greater as 0.7, the deflection shows more or less a strong increasing tendency, depending on the mass and bending stiffness ratios. Also in Fig. 7 it can be observed the same behavior as in Fig. 3: the deflection increases with mass ratio and decreases with bending stiffness ratio.

A convergence analysis is also performed taking for the dynamic deflection with a Ritz approximation of 1, 3 and 5 terms. In Fig. 8, the time history of bending moment at the mid-span of

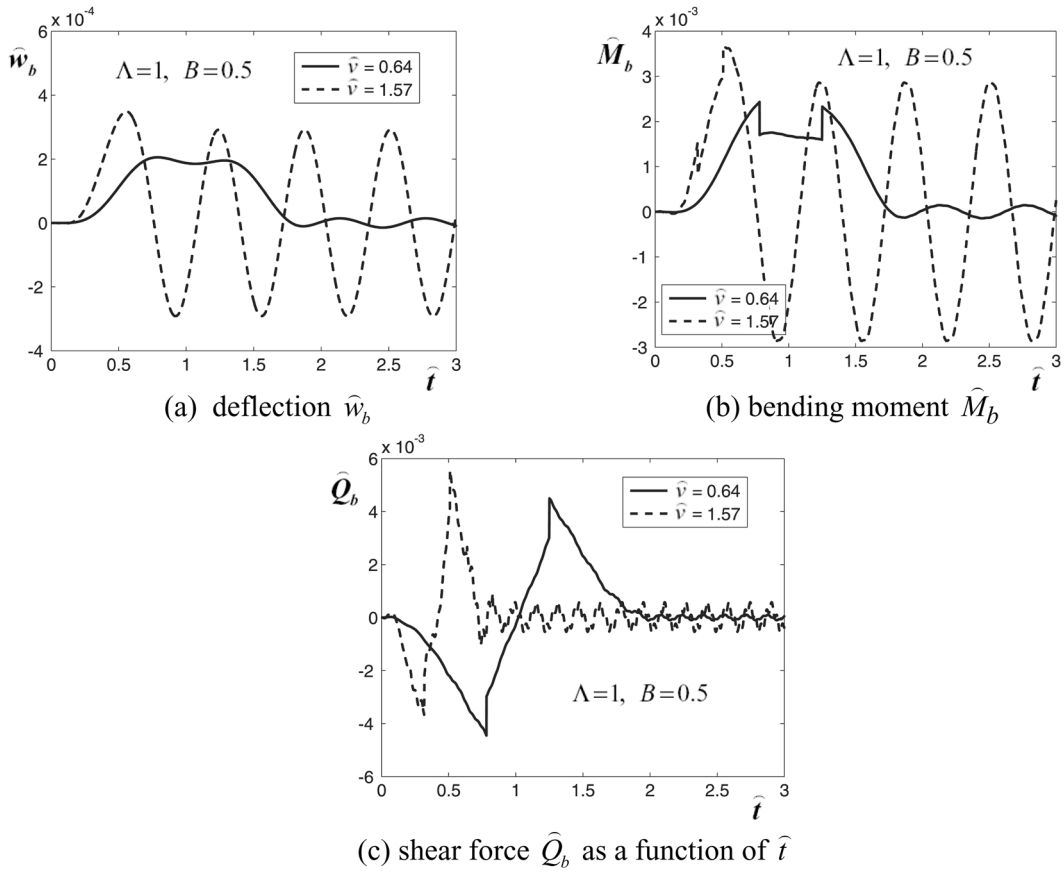


Fig. 6 The response of the bridge at the mid-span for $\Lambda = 1$, $B = 0.5$ and $\hat{v} = 0.64$, $\hat{v} = 1.57$

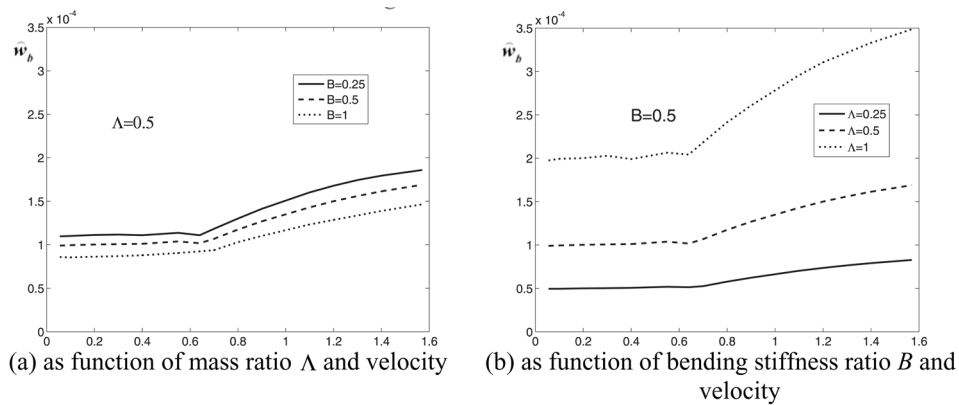


Fig. 7 The maximum deflection of the bridge

the bridge is plotted considering the approximated solution with 1, 3 and 5 terms. It can be observed that the solution with 3 and 5 terms deliver similar results, while the solution with 1 term delivers

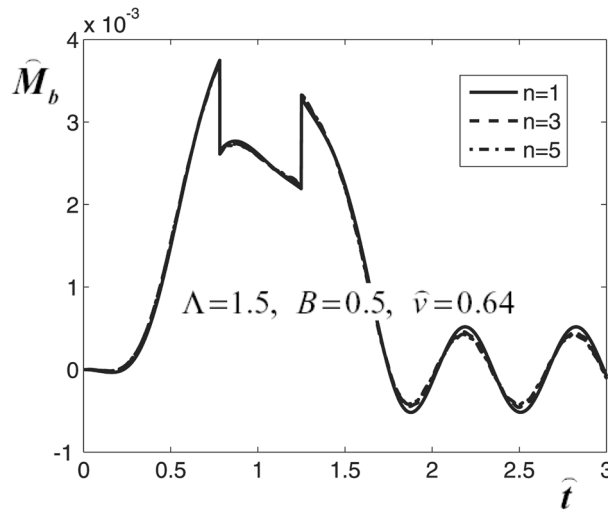


Fig. 8 Convergence of the bending moment at the mid-span of the bridge as a function of \widehat{t}

increased values of the time history. It can be concluded that the approximated solution with 5 terms furnishes satisfactory results.

5. Conclusions

As can be observed in Figs. 3, 4 and 5, the deflection, bending moments and shear forces of the bridge increase with mass ratio Λ , but decrease with bending stiffness ratio B . This means that considering the stiffness of the train leads to a lower overall strength of the bridge. When a rigid interface as a connection between bridge and train is considered, the bending moments and shear forces in the bridge show a jump at the location of the front and end of the train, the amount of this jump increases with a growing B . These traveling jumps, on the other side, indicate a high local strength in the cross-sections that are traversed by the both ends of the train. In a detailed modeling with a non-rigid interface, the concentrated loads at the front of the train would be represented by pressure concentrations.

Acknowledgements

The support of the authors E. Cojocaru and H. Irschik by the ACCM – Austrian Center of Competence in Mechatronics is gratefully acknowledged.

References

Baker, W.E., Westine, P.S. and Dodge, F.T. (1991), *Similarity methods in engineering dynamics. Theory and practice of scale modelling*, Revised Edition, Elsevier Science Publ, Amsterdam.

- Cojocar, E.C., Foo, J. and Irschik, H. (2004), "Quasi-static response of a Timoshenko-beam loaded by an elastically supported moving rigid beam", *Technische Mechanik*, **24**(2), 79-90.
- Cojocar, E.C., Irschik, H. and Gatringer, H. (2004), "Dynamic response of an elastic bridge due to a moving elastic beam", *Comput. Struct.*, **82**(11-12), 931-943.
- Cojocar, E.C., Irschik, H. and Schlacher, K. (2003), "Concentrations of pressure between an elastically supported beam and a Timoshenko-beam", *J. Eng. Mech.*, **129**(9), 1076-1082.
- Esmailzadeh, E. and Ghorashi, M. (1995), "Vibration analysis of beams traversed by uniform partially distributed moving masses", *J. Sound Vib.*, **184**(1), 9-17.
- Fryba, L. (1996), *Dynamics of railway bridges*, Thomas Telford, London.
- Fryba, L. (1999), *Vibration of solids and structures under moving loads*, Thomas Telford, London.
- Greco, A. and Santini, A. (2002), "Dynamic response of a flexural non-classically damped continuous beam under moving loadings", *Comput. Struct.*, **80**(26), 1945-1953.
- Hirsch, M.W. and Smale, S. (1974), *Differential equations, dynamical systems, and linear algebra*, Academic Press, Inc., San Diego.
- Kucharski, T. (2000), "A method for dynamic response analysis of time-variant discrete systems", *Comput. Struct.*, **76**(4), 545-550.
- Lee, H.P. (1996), "The dynamic response of a Timoshenko beam subjected to a moving mass", *J. Sound Vib.*, **198**(2), 249-256.
- Li, J. and Su, M. (1999), "The resonant vibration for a simply supported girder bridge under high-speed trains", *J. Sound Vib.*, **224**(5), 897-915.
- Majka, M. and Hartnett, M. (2008), "Effects of speed, load and damping on the dynamic response of railway bridges and vehicles", *Comput. Struct.*, **86**(6), 556-572.
- Maple On-line Manual - Version 9.5.
- MatLab On-line Manual - Version 6.5.
- Museros, P., Romero, M.L., Poy, A. and Alarcon, E. (2002), "Advances in the analysis of short span railway bridges for high-speed lines", *Comput. Struct.*, **80**(27-30), 2121-2132.
- Pesterev, A.V., Yang, B., Bergman, L.A. and Tan, C.A. (2003), "Revisiting the moving force problem", *J. Sound Vib.*, **261**(1), 75-91.
- Xia, H., Zhang, N. and De Roeck, G. (2003), "Dynamic analysis of high speed railway bridge under articulated trains", *Comput. Struct.*, **81**(26-27), 2467-2478.
- Yang, Y.B. and Lin, C.W. (2005), "Vehicle-bridge interaction dynamics and potential applications", *J. Sound Vib.*, **284**(1-2), 205-226.
- Yang, Y.B. and Wu, Y.S. (2001), "A versatile element for analyzing vehicle-bridge interaction response", *Eng. Struct.*, **23**(5), 452-469.
- Yau, J.D. (2009), "Vehicle/bridge interactions of a rail suspension bridge considering support movements", *Interact. Multiscale Mech.*, **3**(2), 263-276.
- Zhang T. and Zheng, G.T. (2010), "Vibration analysis of an elastic beam subjected to a moving beam with flexible connections", *J. Eng. Mech.*, **136**(1), 120-130.
- Zhang, Q.L., Vrouwenvelder, A. and Wardenier, J. (2001), "Numerical simulation of train-bridge interactive dynamics", *Comput. Struct.*, **79**(10), 1059-1075.
- Ziegler, F. (1991), *Mechanics of solids and fluids*, Springer-Verlag, Inc., New York.